Q. J. R. Meteorol. Soc. (2002), **128**, pp. 47–73

Density currents in shear flows: Effects of rigid lid and cold-pool internal circulation, and application to squall line dynamics

By MING XUE*
University of Oklahoma, USA

(Received 19 January 2001; revised 30 May 2001)

SUMMARY

Idealized density current models that contain a rigid lid, developed in previous studies, are evaluated. It is shown, through numerical experiments, that a realistic stable layer placed at the level of the rigid lid acts very much like a rigid lid, in confining the environmental flow to the levels below and in controlling the behaviour of density currents that propagate in the flow. When this stable layer is replaced by a neutrally stable layer, the behaviour of the density current is very different. These results support the hypothesis that in the atmosphere, the tropopause or a tropospheric inversion layer acts much like a rigid lid in the idealized density current models, and the solutions of these models are applicable to organized quasi-two-dimensional convective systems such as squall lines in the atmosphere.

The effects of cold-pool internal circulations on density current behaviour are also examined. When a single circulation is present initially inside the cold pool, the direction of circulation that gives rise to a smaller shear across the density interface leads to a smoother interface and a much more steady density current head. Large-amplitude eddies develop along the interface when the direction of circulation is reversed. When two layers of shear are initially present inside the cold pool, the flow pattern inside the cold pool tends to be dominated by the circulation of the lower layer. In this case, the behaviour of the density interface and density current head depends on more than just the initial cross-interface shear.

The overall flow pattern in the density current, in which the cold-pool circulation contains rearward flows at the ground level, bears a close similarity to that found in mature squall line systems, as shown by comparisons with a simulated squall line. When the cold pool in a squall line is defined in terms of the equivalent potential temperature, the solutions of idealized density currents in sheared flows become more readily applicable to squall lines.

KEYWORDS: Cold pool shear interaction

1. INTRODUCTION

It is generally recognized that the interaction between the environmental shear and the cold pool of a thunderstorm outflow (density current) plays an important role in supporting long-lived squall lines (Moncrieff 1978; Thorpe *et al.* 1982, TMM82 hereafter; Rotunno *et al.* 1988, RKW88 hereafter; Fovell and Ogura 1988; Xue 1990; Moncrieff 1992). Density currents also occur in the form of sea-breeze fronts (e.g. Simpson *et al.* 1977) and the gust fronts associated with cold-frontal rainbands (e.g. Carbone 1982). Recent detailed observational studies further revealed the importance of density current type sea-breeze and cold-outflow fronts in the initiation and organization of convection (e.g. Weckworth and Wakimoto 1992; Atkins *et al.* 1995).

To improve our understanding of the interaction between density currents and their environment, nonlinear, two-fluid steady-state models with an increasing degree of realism have been developed in recent years, by Xu (1992, X92 hereafter), Xu and Moncrieff (1994, XM94 hereafter), Liu and Moncrieff (1996a), Xue *et al.* (1997, XXD97 hereafter), and Xue (2000, X2000 hereafter). An idealized three-fluid model was also considered in Moncrieff and So (1989). Compared to the classic inviscid density current model of Benjamin (1968), these models considered additional elements: (i) constant and non-constant environmental shear, (ii) internal cold-pool circulation, (iii) negative vorticity generation associated with energy loss along the interfacial layer between the density current and its environment, and (iv) density stratification and latent

* Corresponding address: School of Meteorology, University of Oklahoma, 100 East Boyd Street, Norman, OK 73019, USA. e-mail: mxue@ou.edu

heating. These idealized models show, through mathematical analyses, how the depth, propagation speed and shape of the density current are controlled or influenced by the environmental shear and cold-pool strength. The results from these rather idealized theoretical models have been validated, as far as is possible, by carefully designed high-resolution numerical experiments (e.g. Xu *et al.* 1996; Liu and Moncrieff 1996b; XXD97; X2000).

As pointed out in XXD97 and discussed further in X2000, the density currents in most of the earlier studies are subject to a potentially important limitation: the flow is restricted by a rigid upper boundary. This rigid-lid assumption makes the theoretical treatment viable because the top boundary of the problem is a streamline that can be pre-determined from environmental conditions. Typically, the presence of this rigid lid forces the flow above the density current to run through a narrow channel, thereby reducing the pressure (through the Bernoulli effect) in the region. The reduced pressure often contributes significantly to the support of deep density currents. XXD97 and X2000 suggested that in the real atmosphere a strong inversion layer or the tropopause may act as a rigid lid in channelling the flow underneath, therefore the results from the idealized density current models with a rigid lid is applicable to the atmosphere. When this rigid lid is replaced by a stable layer, internal gravity waves are forced in the stable layer by disturbances from below. The gravity-wave solutions have to be coupled with the density current solution below, making theoretical treatment difficult. In this paper, we resort to a numerical model for the answer. A set of numerical experiments is conducted in which a stable layer replaces the rigid lid of a previously studied density current in a sheared flow, and it is found that the density current solution below it is only quantitatively different from those under a rigid lid. The solution is very different when this stable layer is removed.

When the tropopause acts like a rigid lid, the atmospheric density current in the form of thunderstorm outflow (defined in terms of the potential temperature deviation from the environment) seldom reaches more than a third of the tropospheric depth. This is related to the typical thermodynamic structure in the vertical, hence the limit in cold-air supply. As a result, the real atmospheric density currents tend to be highly turbulent because their height is far below that required for the steady-state solution. To examine this issue, XXD97 conducted an experiment (their experiment SLSA), where the environmental shear is strong enough to support a deep current having a steep frontal slope, while the cold-air supply is insufficient for it to reach the steady-state depth. It was found that, even though the flow was highly turbulent and the cold pool was shallow, the numerical solution still exhibited a branch of deep jump-type flow, with the envelope of cold air and frontal slope more or less agreeing with the steady-state solution (see Fig. 12 of XXD97). The results suggest that even in the cases where a steady-state solution cannot be reached due to the lack of cold-air supply, the theoretical solution of the density current depth and speed still offer very useful guidance on the overall flow behaviour.

The previously studied density current models can be made more applicable to quasi-two-dimensional (2-D) atmospheric convective systems, such as squall lines, if we generalize the two-fluid models to include any flows with fluids of different densities. In a well-established squall line system (see, for example the conceptual model of TMM82 in Fig. 1), we can consider that the entire colder (defined in terms of equivalent potential temperature because the convective region is saturated) descending branch rear-to-front inflow together with the rotor in the head region constitutes the density current. *The density difference and the dynamic (pressure-gradient) force balance across the flow interface* (thick dashed line in Fig. 1), *together with Bernoulli energy conservation along*

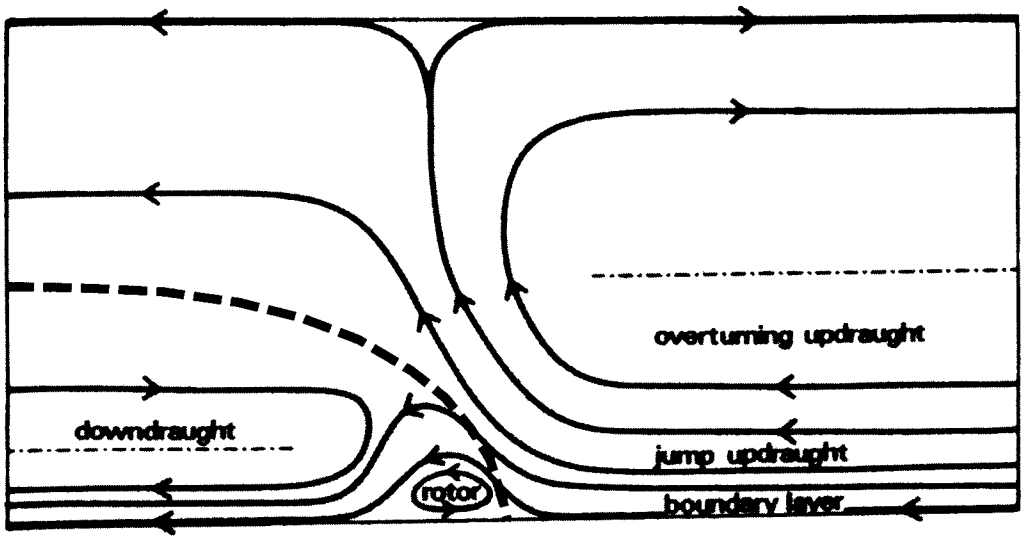

Figure 1. A conceptual model of the two-dimensional squall line of Thorpe *et al.* (1982; reproduced here with an extra-thick dashed line indicating the interface between updraught and downdraught circulations). It can be said that the system is made up of two main types of fluid: one is the warmer, positively buoyant air feeding the updraught, classified as overturning and jump branches by Thorpe *et al.*; the other is the relatively cold, negatively buoyant air that forms the rotor and downdraught circulation. The warmer and colder masses of air are approximately separated by an interface shown as a thick dashed line. In this paper, we consider that the colder mass of air constitutes a generalized density current, and the downdraught and rotor circulations are part of the density current internal circulation.

the streamlines, determine the overall (quasi-steady) flow structure as they do the density current. In this sense, the results of our idealized two-fluid density current models can be extended to explain the squall line dynamics, at least qualitatively.

In mature squall line systems, the circulation associated with the downdraught branch and the rotor circulation in the head region of the density current/cold pool are common features. In most previous studies the effect of the circulation inside the density current is neglected. Xu and Moncrieff (1994) included a cold-pool circulation with constant vorticity in their idealized (inviscid two-fluid) steady-state model of a density current propagating into a flow with uniform vertical shear. They found that, in comparison with the environmental shear, the strength of the cold-pool internal circulation has only a small quantitative effect on the solution of the current (see their Fig. 2), while the direction of the circulation was found to have no bearing on the solution. A counter-clockwise internal circulation associated with positive vorticity has exactly the same effect on the solution as a clockwise circulation. The original idealized density current model for a uniform-shear environment has since been generalized for non-constant environmental shears and verified by numerical experiments (XXD96, XXD97, and X2000). Since the solutions of the latter are obtained from the same set of physical principles, we expected that the finding of XM94 remains qualitatively valid for the idealized models with non-constant shear. XM94's results, however, clearly depend on the assumption that the flow system is inviscid. The idealized models neglect the frictional effect between the two fluids even though shear there is usually large. In a real world, as well as in numerical experiments, the development of Kelvin-Helmholtz (KH) eddies at the interface and the resultant turbulent mixing clearly depends on the cross-interface shear. For this reason, the direction of the internal circulation is expected to

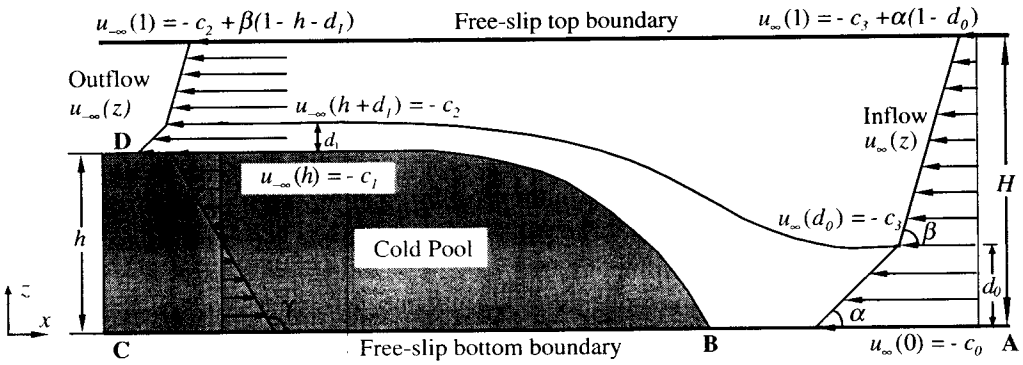

Figure 2. Schematic of the steady-state model of a density current circulation in an environmental flow with two layers of constant shear. The remote system-relative inflow and outflow are indicated by $u_{\infty}(z)$ and $u_{-\infty}(z)$, respectively, and h is the depth of the density current. Inside the cold pool a circulation with constant vorticity γ is shown. Other variables are defined in the text.

affect the behaviour of the density current, perhaps in a significant way. Understanding such effects through numerical experiments is another purpose of this paper.

In the following, we first summarize the basic principles used by, and the key and relevant results from, the previous theoretical models. Section 3 discusses the design of numerical experiments for density currents, and section 4 presents results from these experiments together with a discussion. To further illustrate the applicability of the density current model results to squall line systems, we present in section 5 results from a realistic squall line simulation, and compare the key flow features in the simulated squall line with those in density currents. Finally, a summary with further discussion is given in section 6.

2. IDEALIZED DENSITY CURRENTS IN A TWO-LAYER SHEAR FLOW

In this section, we briefly discuss the theoretical models of idealized 2-D density currents. X2000 considers an idealized steady-state density current in an environmental flow with two constant-shear layers under a rigid lid. The model, with an additional cold-pool circulation with constant vorticity γ, is illustrated in Fig. 2. The variables in this model are non-dimensionalized using the following scaling:

$$(x, z) \leftarrow (x, z)/H,\ (u, w) \leftarrow (u, w)/U,\ p' \leftarrow p'/(\rho_0 U^2),$$

where the variables on the left-hand side of the arrow are non-dimensional.

In Fig. 2, the shaded area indicates the cold pool of an idealized density current. The flow is assumed to be in a steady state in a reference frame moving with the current. x and z are the horizontal and vertical coordinates; u and w are the horizontal and vertical velocities, respectively; H is the depth of the domain bounded by two rigid boundaries; $U \equiv (gH\Delta\rho/\rho_0)^{1/2}$ is the velocity scale; g is the acceleration due to gravity; $\Delta\rho \equiv \rho_1 - \rho_0$ is the density difference between the denser fluid inside the cold pool (ρ_1) and the lighter fluid outside (ρ_0); and $p' \equiv P - P_0$ is the perturbation pressure, which is the difference between total pressure P and reference pressure P_0. The reference pressure P_0 is the unperturbed pressure in the upstream inflow associated with constant density ρ_0, where P_0 satisfies the hydrostatic relation $P_0 = g\rho_0(H - z)$. Viewed in a framework moving with the density current front, the low-level

environmental flow moves towards the head from the right (the upstream). The flow outside the cold pool is separated into two layers, each with a constant vorticity. This constant vorticity dictates that the horizontal flow at the far downstream has the same shear as that at the far upstream in both the upper and lower layer. The circulation inside the cold pool, considered in this paper, is assumed to have a constant vorticity, γ.

In Fig. 2, α and β are, respectively, the constant lower and upper-level shears of the environmental inflow. $d_0 (0 \leq d_0 \leq 1)$ is the depth of the lower layer in the far upstream, and $c_0 (> 0)$ the constant inflow speed (absolute value) at the lower boundary; d_1 is the depth of the lower shear layer above the cold pool in the far downstream, and $c_1 (> 0)$ is the speed of outflow above the cold pool. Finally, $h (0 < h < 1)$ is the depth of the density current head. Without considering the cold-pool internal circulation (as in X2000), the flow is fully described by seven non-dimensional control parameters, α, β, d_0, c_0, d_1, c_1, and h.

Following the discussion of Benjamin (1968), the remote system-relative environmental inflow and outflow are constrained by mass continuity, vorticity conservation, flow–force balance and the conservation of Bernoulli energy along streamlines. It can be shown that only three of the seven parameters are independent, and physical solutions can be found given any three of these parameters. Xue (2000) discusses the cases where the shears of inflow (α and β) and the height of the inflow layer interface (d_0) are prescribed. Once these are given, the ground-level inflow speed (c_0), the depth of the density current (h), the outflow speed (c_1) and layer depth (d_1) are determined by the model. A numerical procedure is used to find the solutions for h, c_0, c_1 and d_1 and the results are plotted as curves. When the cold-pool circulation is considered, the shear (vorticity) of this circulation becomes an additional external parameter. Since these eight parameters describe the flow away from the density current head region where the flow is horizontal, the results from the aforementioned procedure describe the far-field solutions.

According to X2000, the density current becomes deeper and propagates faster relative to the surface environmental flow as the shear in the low-level inflow increases from negative through positive values. The effect of the upper-level shear is similar—increased upper-level shear supports a deeper density current. When the shears in both layers are equal, the solution reduces to that of X90 for constant-shear inflow and to that of Benjamin (1968) when the shear in both layers is zero. In general, when the overall shear in the inflow is positive, the density current depth is more than half of the vertical channel depth.

The effects of cold-pool internal circulation on the density current in a constant environmental shear were examined in XM94. It was found that the internal circulation of constant vorticity has only a relatively small (typically less than 10%) quantitative effect and the effect is independent of the direction of circulation.

Apart from the far-field solutions, the flow structure near the front is also important. In the case of thunderstorm outflow, the shape of the front has a direct influence on the vertical orientation of low-level updraught. An upshear-tilted updraught allows condensed water to be downloaded underneath the updraught without interrupting the low-level inflow, thus long-lived squall line type convection can be maintained (e.g. TMM82; RKW88).

Von Karman (1940) and Benjamin (1968) showed analytically that the angle at the stagnation point between the density front and the horizontal is 60° for an idealized inviscid density current in a uniform (non-sheared) environmental flow with a free-slip lower boundary condition. It was further shown in X92 and XM94 that this 60° angle is independent of the inflow shear and cold-pool circulation. The shape of the frontal interface away from the lower boundary is determined by the continuity condition of

pressure across the interface, and the solution can be obtained numerically (Xu *et al.* 1992). According to X92 and XM94, when the positive inflow shear is very strong, the frontal interface slope can become steeper than 60° at mid-depth ($z = h/2$). It is expected that these findings can be extended to the model with two layers of inflow shear.

In the following two sections, we discuss the design of and results from density current numerical experiments.

3. THE DESIGN OF NUMERICAL EXPERIMENTS FOR DENSITY CURRENT

As in XXD97 and X2000, a modified version of the Advanced Regional Prediction System (ARPS, Xue *et al.* 1995; Xue *et al.* 2000) is used for our density current simulations. The ARPS is used in its simplest dry 2-D mode with no physics. To facilitate direct comparison of numerical results with the theoretical solutions, the Boussinesq approximation is assumed. The base-state density, ρ_0, and potential temperature, θ_0, are set to be constant. For the experiments with a rigid top lid, rigid free-slip conditions are applied at both top and bottom boundaries. For those with a stable upper layer, a wave-radiating upper-boundary condition is used (Xue *et al.* 2000). Open conditions are also used at the upstream and downstream boundaries. More details of the model set-up for rigid-lid cases can be found in XXD97 and X2000.

As in earlier studies, we do not include subgrid-scale turbulence parametrization, but rely on the high spatial resolution to resolve the turbulent eddies often found to the rear of the current head. We apply a small amount of horizontal computational mixing/diffusion to the velocity fields only. We avoid applying mixing in the vertical for fear of affecting the vertical wind profile. The monotonic flux-corrected transport scheme of Zalesak (1979) is used to advect the potential-temperature field.

The equations actually solved by the model are those for u, w, p' and perturbation buoyancy b, in non-dimensional form, as given in XXD97 (their Eq. (3.1)). The same scaling parameters as in XXD97 are used here for non-dimensionalization of the model equations, except for the definition of H.

Length scale:	H (the height of the rigid lid or the bottom of the upper stable layer)
Velocity scale:	$U \equiv (gH\Delta\rho/\rho_0)^{1/2}$
Pressure scale:	$P \equiv \rho_0 U^2 = gH\Delta\rho$
Time scale:	$T \equiv H/U$
Buoyancy scale:	$B \equiv g\Delta\rho/\rho_0 = g\Delta\theta/\theta_0$

In the dimensional ARPS model, we choose for convenience $H = 1$ km, $\Delta\theta = 3$ K, $\theta_0 = 300$ K, $g = 10$ m s^{-2}. The other derived scaling parameters are $U = 10$ m s^{-1}, $P = 120$ Pa and $T = 100$ s. Since our results will be presented and discussed in non-dimensional space, the results are not limited to shallow domains.

The density current in the numerical model is generated by placing an initially static block of cold air ($b = -1$) in the middle portion of an elongated computational domain of size $38.3 \times D$ non-dimensional units, consisting of $767 \times (80 \times D + 1)$ grid points. Here $D = 1$ or 3. Therefore, the grid spacings are $\Delta x = 0.05$ and $\Delta z = 0.0125$ in the horizontal and vertical directions, respectively. The initial cold block is specified to be more than eight non-dimensional units in width, and is in most cases able to supply

sufficient cold air to achieve and maintain a quasi-steady density current. The initial shape of the cold pool is specified in the same way as in XXD97 (cf. their Eq. (3.3)). The interface has a slope of 60° at the frontal nose.

To examine the effect of a rigid top lid versus a stable layer, we conducted a set of three experiments, listed as LID0, LID1 and LID2 in Table 1. Experiments LID1 and LID2 are based on control experiment LID0, which is essentially experiment SLS in XXD97 (see Table 1 in XXD97). In this experiment: a rigid lid is placed at non-dimensional height $D = 1$, the shear in the inflow is confined to the low-level depth of ($d_0 =$) 0.2, and the shear magnitude is a relatively large value of ($\alpha =$) 3. No cold-pool internal circulation is considered in this set of experiments, i.e. $\gamma = 0$. The theoretical model predicts a deep density current of depth ($h =$) 0.77 (see Fig. 2 of XXD97). The initial flow for the experiment is specified in the same way as in XXD97, i.e. the upstream and downstream flow is determined from the specified parameters and the corresponding theoretical model solutions, and the interior flow is obtained by solving a steady-state vorticity equation expressed in terms of the stream function. The top-boundary condition for the stream function is known from the upstream boundary condition. The stream function is constant following the upstream lower boundary and along the density current interface. This initial set-up closely resembles the steady-state solution of the theoretical model.

Experiments LID1 and LID2 are variations of LID0. In LID1, the rigid lid in LID0 is removed and a stable layer of depth two and a static stability (N) of 2×10^{-2} s^{-1} (roughly corresponding to the stability of an isothermal layer) is placed above the original channel of depth unity. The purpose here is to examine how much this stable layer acts like a rigid lid, and if the density current solution is significantly altered by this change. This experiment employs a wave-radiating top-boundary condition at $z = 3$, allowing gravity waves to exit the boundary freely. In experiment LID2, the stable layer in LID1 is replaced by a neutral layer of the same depth and a rigid lid is placed at $z = 3$. In both experiments, the initial cold block is the same as in LID0, and the zero-shear upper-level inflow is extended to the top of the domain. The initial flow near and above the cold block is again obtained from the vorticity equation, but this time with the constant stream-function upper-boundary condition specified at $z = 3$. Significant initial flow adjustment is expected due to the presence of a stable layer.

Experiment LID2 is essentially a case of a density current propagating in a neutrally stable environmental flow of depth three. If we rescale the problem using the new domain depth of three, then the low-level inflow shear is about 0.067 in depth (in terms of the total domain depth). According to the theoretical models of XXD97, the steady-state density current depth should be more than 0.5 of the domain depth, which, in terms of our current scaling, gives a depth of more than 1.5. The initial depth of the cold block is 0.77 in LID2 and is specified according to the solution with a domain depth of unity, therefore significant adjustment is expected. Because the initial depth is significantly lower than the expected depth therefore the cold air supply is likely to be insufficient, and a steady-state solution may not be able to become established. This is a situation that is similar to experiment SLSA in XXD97.

The other set of experiments examines the effects of internal circulation inside the density current or cold pool. We introduce such a circulation by specifying the far-field (downstream) flow shear. We assume that the net inflow into the density current and therefore the vertically averaged (through the depth of the current) flow speed at the far downstream is zero. From Fig. 1, we can see that both positive ($du/dz > 0$) and negative circulations are possible inside the generalized density current of a convective system, with the negative circulation typically associated with the rotor circulation and

TABLE 1. INITIAL SETTINGS AND SIMULATED PARAMETER VALUES FOR THE NUMERICAL EXPERIMENTS WITH DENSITY CURRENTS.

Experiment	Specified parameters				Theoretical/simulated values	
	α	β	γ	D	h/simulated h	c_0/simulated c_0
LID0	3	0	0	1	0.77/0.76	0.78/0.79
LID1	3	0	0	3, stable upper layer	0.77/0.78	0.78/0.85
LID2	3	0	0	3, neutral throughout	0.77/1.13	0.78/0.98
L0U2	0	2	0	1	0.72/0.68	0.97/0.95
ICP1	0	2	1	1	0.72/0.60	0.97/0.96
ICN1	0	2	−1	1	0.72/0.71	0.97/0.98
IC2P2	0	2	2	1	0.72/0.51	0.97/0.95
IC2N2	0	2	−2	1	0.72/0.70	0.97/0.99

Note that the theoretical values listed for ICP1, ICN1, IC2P2 and IC2N2 are those corresponding to L0U2, which does not include any cold-pool internal circulation.

the positive one with the downdraught circulation to the rear. At different stages of a squall line development, one of these may dominate. When the rotor circulation is expanded further to the rear and extends partially beneath the positive downdraught circulation, one obtains a two-layered circulation within the density current, with a layer of positive vorticity located above a layer of negative vorticity. In other cases where the rotor circulation is weak and the rear-to-front inflow jet (see, e.g. the conceptual model of Houze 1989) is fully developed, inside the density current one would expect a negatively sheared layer located above the positively sheared downdraught circulation with rear-to-front inflow in-between (cf. Fig. 1).

We conceptualize the above situations by considering single and double circulations of different directions inside the cold pool, and examine their effects on the behaviour of the density current in a set of four numerical experiments. In experiment ICN1, a single cold-pool internal circulation with negative vorticity of magnitude unity is considered. Experiment ICP1 is the same as ICN1 except for the direction of the internal circulation. These two experiments correspond to the cases of $\gamma = -1$ and $+1$ as illustrated by Fig. 2.

In experiments IC2N2 and IC2P2, two internal circulations are included, corresponding to two layers of shear of opposite signs at the downstream boundary of the density current (see Figs. 10(a) and 11(a)). In IC2N2, the lower layer has negative and upper-layer positive vorticity of magnitude two. IC2P2 is the same except that the internal circulations have opposite directions. The magnitude of two is chosen so that the flow speeds at the ground level and at the density interface are the same as those in the corresponding single-layer cases. Therefore, the cross-interface shear is the same in the single- and double-circulation cases when the flow direction below the interface is the same.

In this second set of (four) experiments, the initial configurations are based on the theoretical model solution for an upper-level shear-inflow case with a rigid lid and zero internal circulation. Inflow shear below 0.2 is zero and above is two. This reference case is considered in X2000 as experiment L0U2 (see X2000 Table 1) and it supports a relatively deep density current. The results from L0U2 are included in Table 1 here. The theoretical depth of the current (without internal circulation) is 0.72 and the model-simulated depth is 0.68.

In the numerical solutions, transient activities are expected to the rear of the current head due to KH instability. When the simulation results are compared with the idealized model, we determine the height of the simulated current at a location where the flow

interface becomes more or less horizontal and KH eddies are insignificant. In the following section, we discuss the results of these numerical experiments.

4. Results of numerical simulations of density current

All numerical simulations are carried out to a non-dimensional time $T = 24$. Ensemble time averages are produced for simulated fields over the period $T = 12$ to $T = 18$ at a sampling interval of 0.5. To avoid spatial smoothing due to the current propagation, the instantaneous fields are translated in x before averaging, so that their frontal noses collocate with the nose at $T = 12$. Instantaneous fields at selected times and the time-averaged fields are shown. All fields shown are non-dimensional unless stated otherwise, and the flow speed is relative to the density current front.

(a) *Rigid lid versus a stable layer*

The results from experiments LID0, LID1 and LID2 are discussed in this section. Figure 3 and Fig. 4 show the flow and dimensional potential-temperature fields from these experiments at non-dimensional times $T = 12$ and 18. Figure 5 shows the corresponding fields averaged over the period from $T = 12$ to $T = 18$.

The simulated density current in LID0 is essentially stationary relative to the grid and the head is in a nearly steady state. The height of the current is estimated to be between 0.75 and 0.78 from $T = 12$ and 18, very close to the theoretical value of 0.77. The ground-level inflow-relative propagation speed is estimated to be 0.79 between $T = 12$ and 18, again very close to the theoretical value of 0.78. Since LID0 is essentially a re-run of experiment SLS in XXD97, Fig. 3(a) and Fig. 5(a) should closely match Fig. 10(a) and Fig. 10(b) in XXD97, respectively, with the small differences being attributed to the use of different advection schemes. Given the very deep density current, the environmental flow is channelled rapidly through a shallow depth above the current, resulting in a large pressure drop over the head due to the Bernoulli effect. This effect is clearly shown in Fig. 6(a). This channelling effect, and the resultant pressure drop, is instrumental in creating a large upward pressure gradient that supports such a deep and quasi-steady density current.

The simulated density current in LID1 is not as nearly stationary as that in LID0. At $T = 12$, the front is located close to $x = 1.5$, and at $T = 18$ close to $x = 2.0$. As a result, the ground-level inflow-relative propagation speed of the front between $T = 12$ and 18 is about 0.85 versus the theoretical value of 0.78, a difference of about 10%. The density current height, measured by the 299 K potential-temperature contour (corresponding to non-dimensional buoyancy of -0.5) in the time-averaged plot (Fig. 5(b)) is about 0.78, very close to the theoretical value 0.77 of the rigid-lid case. The simulated head is not as steady as the rigid-lid case, however, and the KH eddies develop more quickly along the interface and gain large amplitudes (Figs. 3(b) and 4(b)). The obviously new features found in this run are the internal gravity waves in the stable layer forced by the flow and eddy activities below. The forcing is strong enough for wave overturning to occur at $T = 18$ (Fig. 4(b)); in fact, the overturning of isentropes remains evident in the time-averaged plot (Fig. 5(b)). What is equally important to us is that, directly above the current head, the 301 K isentrope that was originally located near the $z = 1$ level has now been pushed up to nearly $z = 1.2$ by flow channelled over the current head. The raised isentropes make for more room for the neutral inflow to pass over the head, resulting in less acceleration there.

The pressure drop due to the Bernoulli effect is subsequently less in LID1, as seen from Fig. 6. The minimum pressure over the head is about -0.35 as compared to -0.42

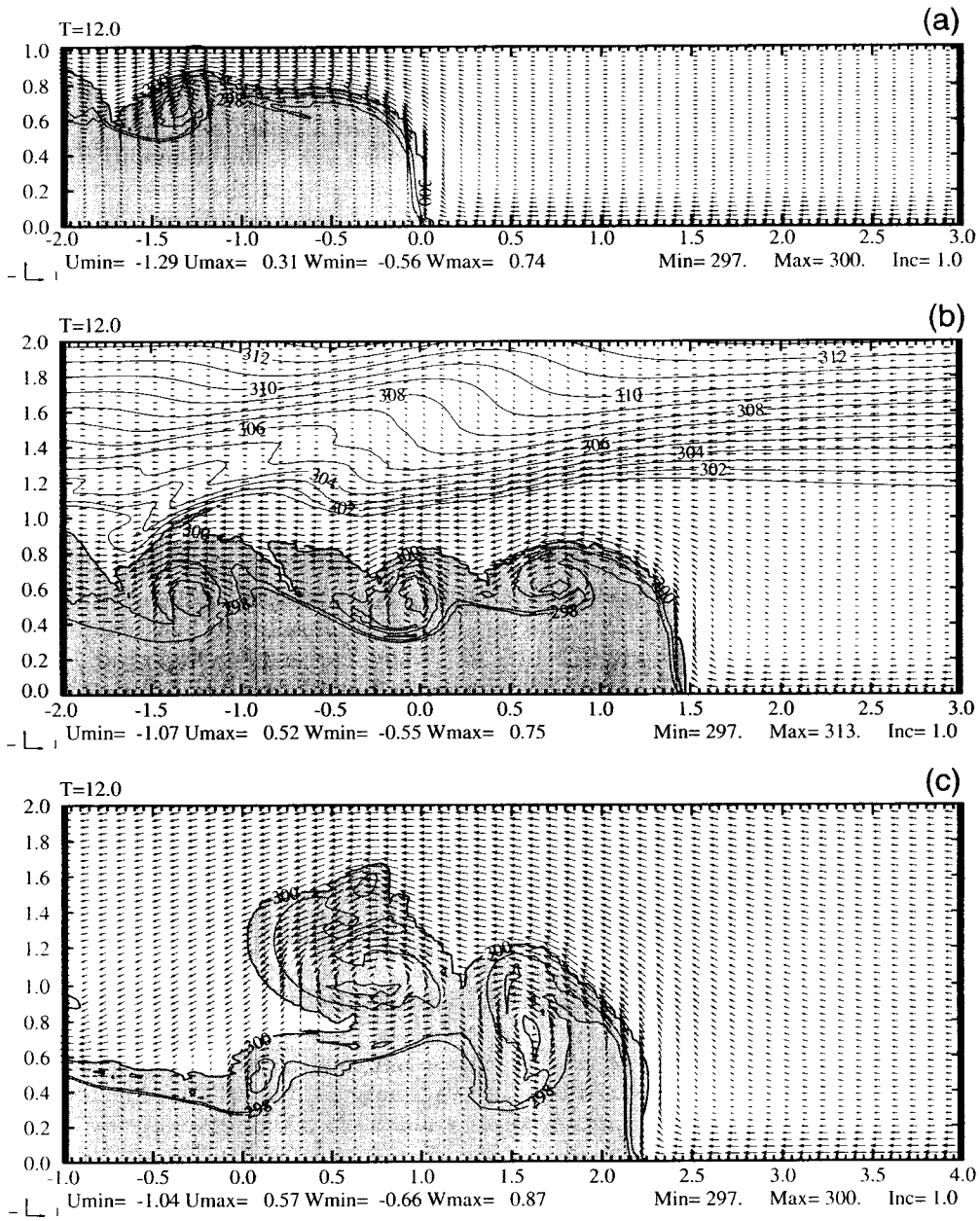

Figure 3. Non-dimensional front-relative velocity vectors and the potential-temperature field (K) at time $T = 12$ (20 minutes model time) in non-dimensional coordinates, for experiments: (a) LID0, (b) LID1, and (c) LID2. The contour interval is 1 K for potential temperature, and areas with potential temperature less than 300 K are shaded. The domain is plotted to the physical scales, and $x = 0$ is located at the initial location of the frontal nose. The horizontal and vertical velocity scales ($u = w = 1$) are shown by the arrow key at the lower-left corner of each plot. Note that a different portion of domain is shown in (c). See text for further details.

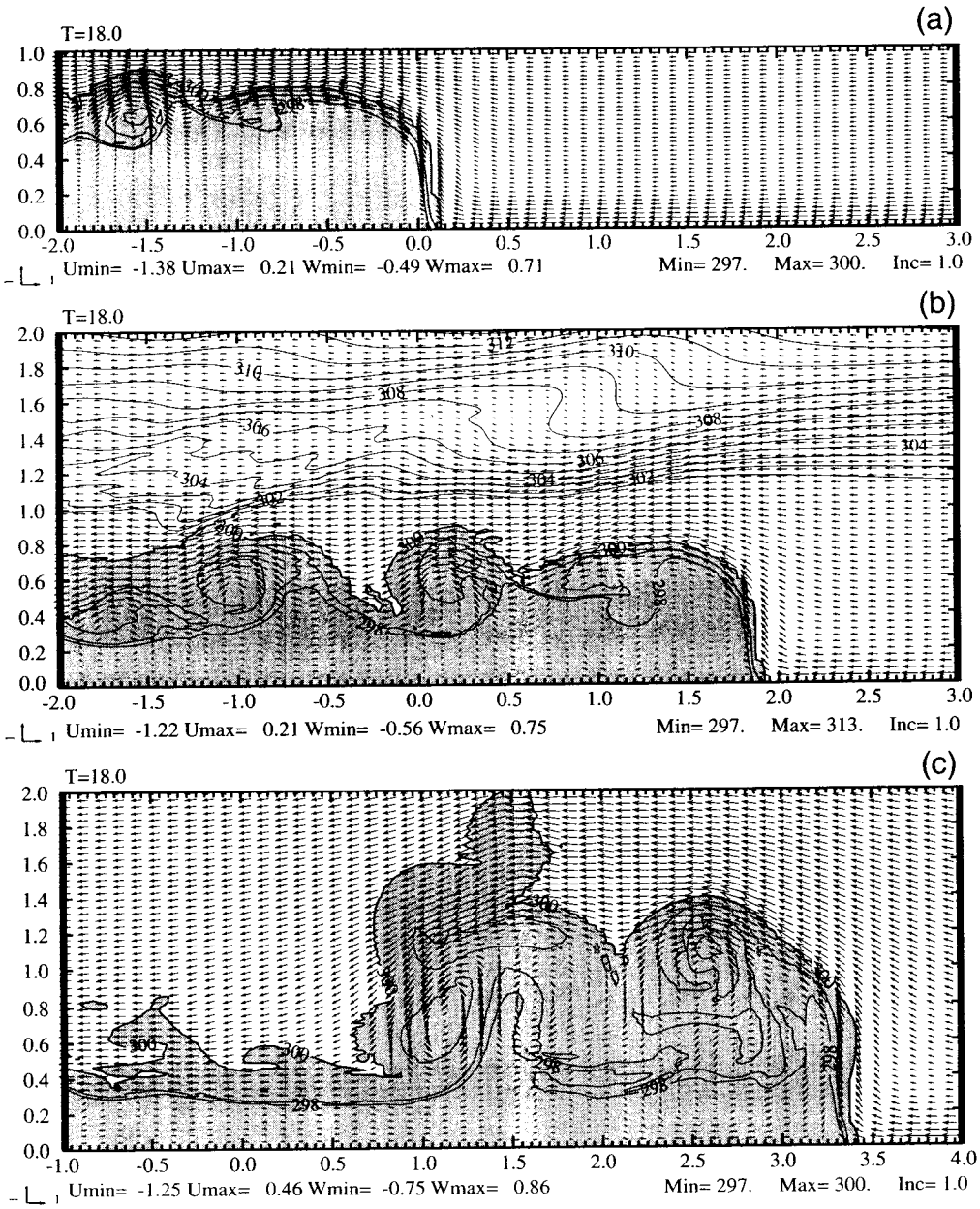

Figure 4. Same as Fig. 3 except that time $T = 18$.

in LID0. This reduced pressure drop should lead to a weaker vertical pressure gradient force, hence a shallower density current. The latter does not seem to be happening, given that the simulated current height is close to or even slightly larger than the theoretical value. This can be explained by the fact that the effective depth of the domain in which the current propagates is increased by almost 20% due to the raised lower boundary of the stable layer. If one re-scales the density current depth by the new increased domain depth of 1.2, the non-dimensional height of 0.78 would be equivalent to 0.65,

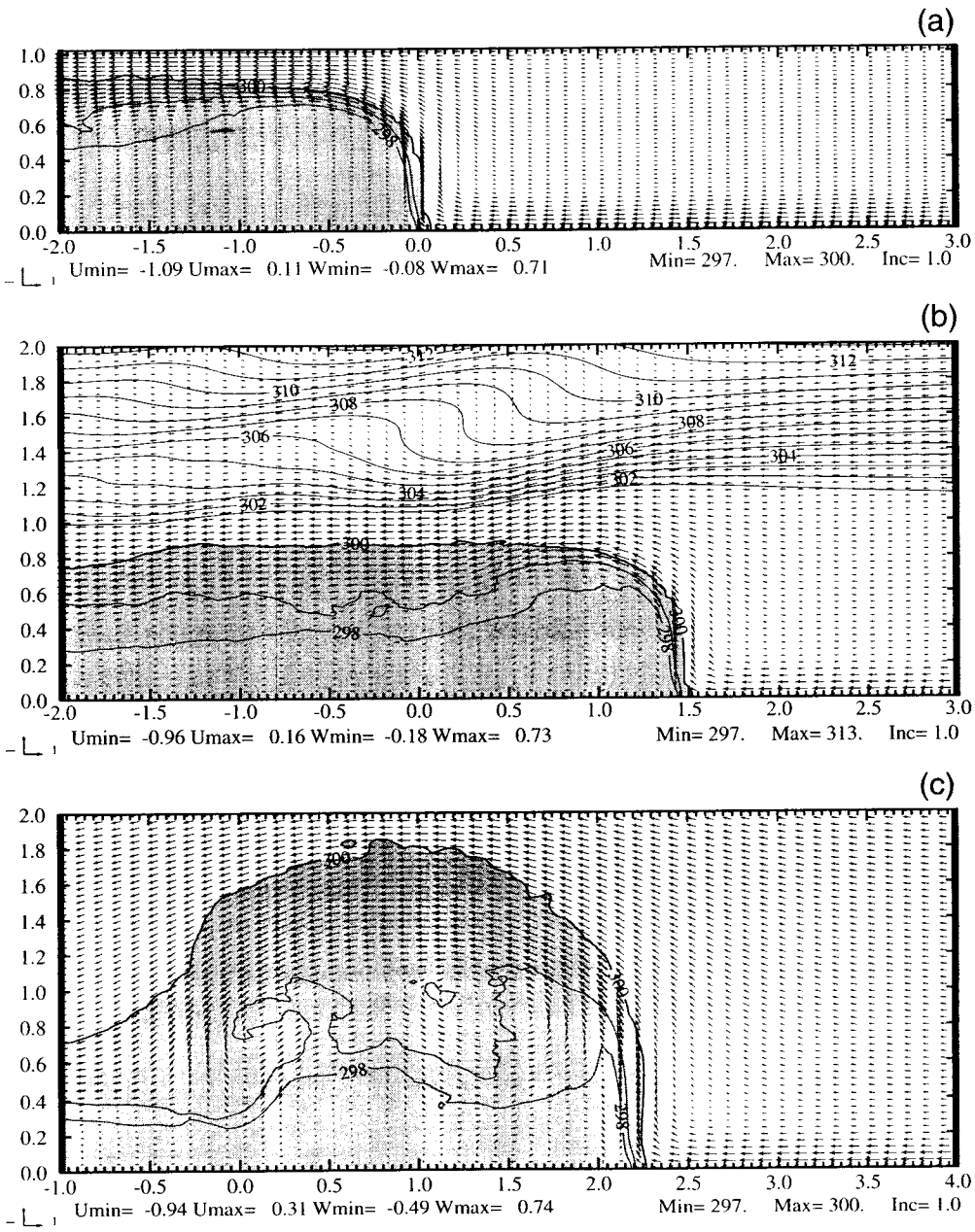

Figure 5. Same as Fig. 3 except that the fields plotted are averaged from time $T = 12$ to 18.

significantly lower than the original theoretical value of 0.78. In other words, for a density current propagating into an environmental flow capped by a layer of strong static stability, the decreased channelling effect above the density current, and hence decreased support from vertical pressure gradient, is roughly compensated by the increased scale depth due to the upward shift of the base of stable layer. The depth of the density current head (based on the original scaling) ends up being very close to that predicted

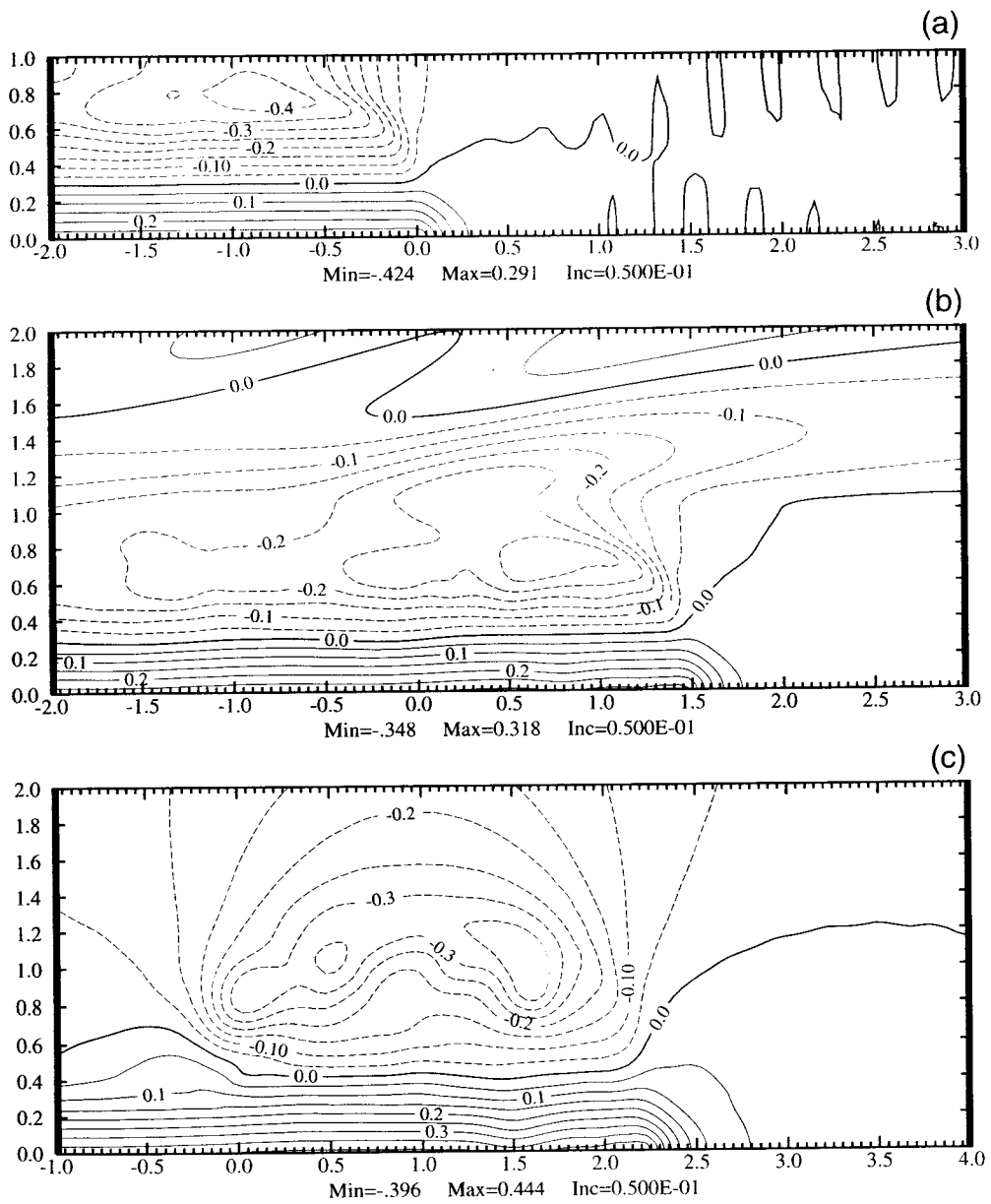

Figure 6. The time-averaged non-dimensional perturbation pressure field for experiments: (a) LID0, (b) LID1, and (c) LID2, corresponding to those in Fig. 5. The contour interval is 0.005.

by a theoretical model with a rigid lid. This is true at least for the inflow configuration considered here.

The speed of the current in this case is found to be about 10% faster than in the rigid-lid case. Again this can be understood quite well by re-scaling the velocity values. Since the velocity scale we need for non-dimensionalization (see section 2) is $U \equiv (gH\Delta\rho/\rho_0)^{1/2}$, a 20% increase in H leads to an approximate 10% increase in

the velocity scale. Using the new velocity scale that is 10% larger, we obtain a non-dimensional propagating speed that is almost exactly the same as the theoretical value. The exact values here should be viewed with some caution, however, because when one changes the scale depth, H, the effective depth of the low-level shear is also changed. Nevertheless, the above arguments should be qualitatively valid. The slightly larger pressure gradient across the frontal nose at the ground level in LID1 is consistent with a slightly deeper current head and less pressure drop above, and therefore with the faster propagation speed.

The results from experiment LID2, in which the rigid lid is in effect extended to $z = 3$, are shown in Figs. 3(c), 4(c) and 5(c). The behaviour of the simulated density current in this case is quite different from the previous two cases; the current head is much more unsteady, and large eddies develop very quickly behind the head region and grow in size. In fact, the interface never reaches a quasi-steady horizontal state in the head region. As a result, the time-averaged field (Fig. 5(c)) shows significant smoothing due to eddy mixing in the potential-temperature field, starting immediately behind the front. In the time-averaged field, the two-degree temperature difference spans a depth of about 1.4, with the negative-buoyancy air reaching a height of 1.9. The current also propagates significantly faster than in the previous two cases, with the ground-level inflow-relative speed being about 0.98, roughly 25% more than that of the LID0 case. As mentioned earlier, this is a case that is similar to experiment SLSA in XXD97. For a channel of depth three, the specified initial cold pool is much lower than the steady-state solution given by the theoretical model. In this case, the inflow has a positive shear of magnitude three and a depth of about 7% of the channel depth, the expected current depth should be more than 0.5 of the channel depth, i.e. more than 1.5. Clearly, the model is trying to establish such a deep current, but because of the lack of sufficient cold-air supply a quasi-steady state cannot be reached. The flow is therefore much more turbulent, but even so, a tendency to establish a deeper cold pool and a deep jump-type updraught is obvious, as was the case in SLSA of XXD97 (e.g. see their Fig. 10).

Furthermore, because of the large space above the cold pool, the channelling effect for the inflow is much weaker, and the pressure drop due to the Bernoulli effect is much smaller. As shown by Fig. 5(c), much of the channelling effect occurs above the 1.2 level where the magnitude of the pressure perturbation is less than 0.3 units (Fig. 6(c)) smaller than those in the previous two cases. The two centres of minimum pressure below this level in Fig. 6(c) are associated with two horizontal eddies seen in Fig. 5(c), due to the dynamic (centrifugal) effect in vortices. The deeper though somewhat diffused cold pool, and the smaller pressure drop aloft, lead to higher pressure underneath the density current. The maximum surface pressure perturbation in Fig. 6(c) is 0.444 versus 0.291 in LID0, and the large cross-frontal pressure gradient causes the front to propagate significantly faster than in the LID0 case.

In summary, the results from experiments LID0, LID1 and LID2 show that a realistic stable layer placed at the level of a rigid lid acts very much like a rigid lid, in confining the environmental flow to the levels below and in controlling the behaviour of density currents that propagate in the flow. For a low-level shear-inflow case examined here, the density current obtained has essentially the same depth as that under a rigid lid (placed at the height of the base of the stable layer), the inflow-relative propagation speed of the current is faster, but the difference is less than 10%. If this stable layer is replaced by a neutrally stable layer under a much higher lid, the behaviour of the density current is very different. The current attempts to reach a much deeper depth consistent with the much deeper channel, and the flow becomes much less steady because of the lack of a sufficient supply of cold air to reach a quasi-steady state. These behaviours can be

quantitatively understood by re-scaling the parameters using the new, modified channel depth.

(*b*) *Effect of density current internal circulations*

In this section, we examine the results from the second set of experiments that include circulations inside the cold pool. Figures 7 and 8 show the fields at $T = 0$ and $T = 18$, respectively, from experiments ICP1 and ICN1, in which a single circulation of positive and negative vorticity, respectively, is specified inside the cold pool at initial time (Fig. 7). Other settings of the experiments are the same as those for experiment L0U2 in X2000, and are specified according to the solution of the corresponding theoretical model. In L0U2, the simulated density current remains essentially stationary relative to the model grid, and its depth is close to the theoretical value (0.68 versus 0.72). Figure 9 shows the time-averaged fields corresponding to those in Fig. 8. It is inferred from the theoretical study of XM94 on inviscid density currents, that the internal circulation should have only a very small effect on the density current, and for the inviscid cases considered there the effect does not depend on the direction of internal circulation.

It is clear that the flow behaves very differently in these two cases. The turbulent eddies along the interface in ICP1 are large and strong, developing quickly along the frontal interface. On the contrary, the interface in ICN1 is rather smooth for a significant distance behind the head region. This interface is also remarkably steady. In fact, this is the closest case we have seen so far to the solution of an inviscid density current considered in the theoretical studies. The interface seen from the time-averaged field (Fig. 9(b)) is almost as sharp as that from the instantaneous one in Fig. 8(b), indicating very little transient activity along the interface. The interface in ICP1 is significantly diffused, however (Fig. 9(a)). Such large differences are obviously due to the difference in the cross-interface shear. In ICP1 the flow below the interface is in an opposite direction, as the strong front-to-rear flow above creates a large shear across the interface and therefore favourable conditions for KH eddies to develop. In ICN1, the flow associated with the internal circulation is in the same direction below as above the interface, reducing the cross-interface shear (even compared with the case without internal circulation), therefore the interface is much more stable with respect to KH instability. The fast rearward advection of any vortices developed along the interface by flows both below and above the interface further reduces the disturbances found in the head region.

The height of the density current, measured by the maximum height of the -0.5 buoyancy contour in the time-averaged field, is about 0.6 for ICP1 and 0.71 for ICN1. The former is significantly lower than the theoretical value of 0.72, mostly due to the diffusive eddy activities near the head. The height in ICN1 is very close to the theoretical value. In fact, it is even closer (0.71 versus 0.68) than the case without internal circulation (L0U2). In both cases, the speed of the current is very close to the theoretical value, with that in ICP1 moving slightly slower and that in ICN1 slightly faster. The difference in both cases is actually smaller than in L0U2. In a sense, by introducing an internal circulation that reduces the cross-interface shear, we obtain a density current in a numerical model that is even closer to the solution of a two-fluid inviscid theoretical density current model. These results further cross-validate our theoretical models and numerical simulations of density currents. The numerical results also show that for realistic flows the direction of the cold-pool circulation does matter.

In the next two experiments, the cold pool contains at the initial time two shear layers having vorticity of opposite signs. The initial flow patterns are shown in

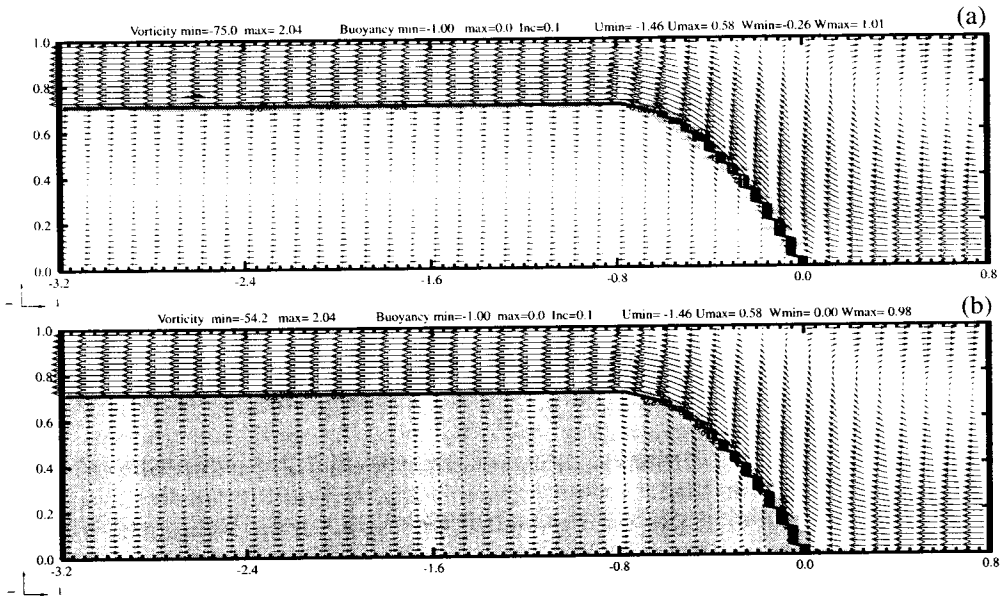

Figure 7. Non-dimensional velocity vector and buoyancy (contour) fields at initial time ($T = 0$), for: (a) experiment ICP1, and (b) ICN1. A single circulation with positive (clockwise) vorticity of unity is specified inside the cold pool at initial time in ICP1 and a single circulation of opposite direction (counterclockwise) in ICN1. Areas with negative vorticity are shaded. For ICP1, negative vorticity appears only at the flow interface at this time.

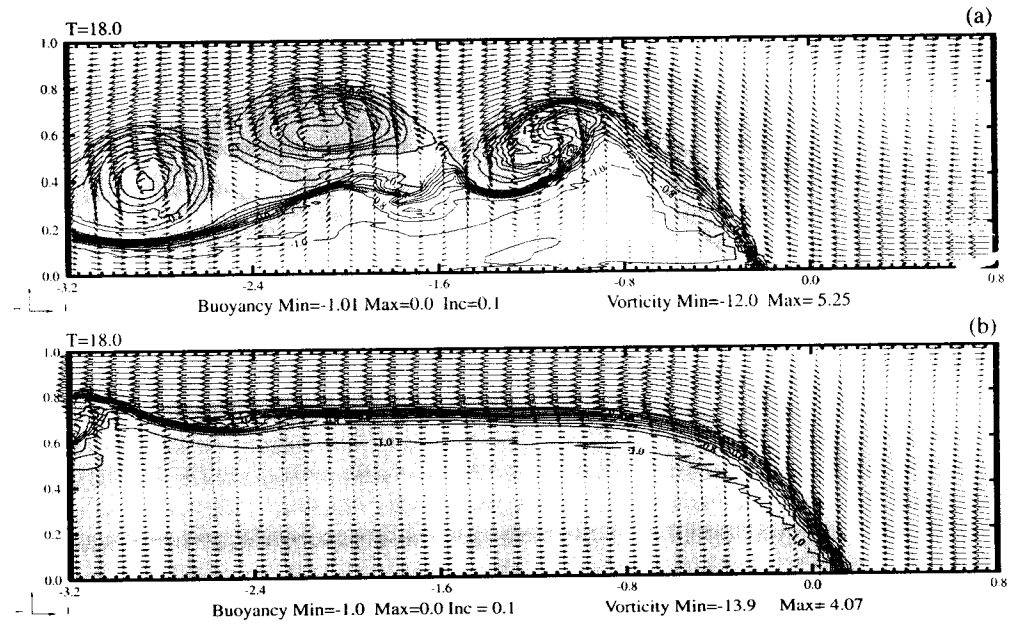

Figure 8. As Fig. 7 but at non-dimensional time $T = 18$.

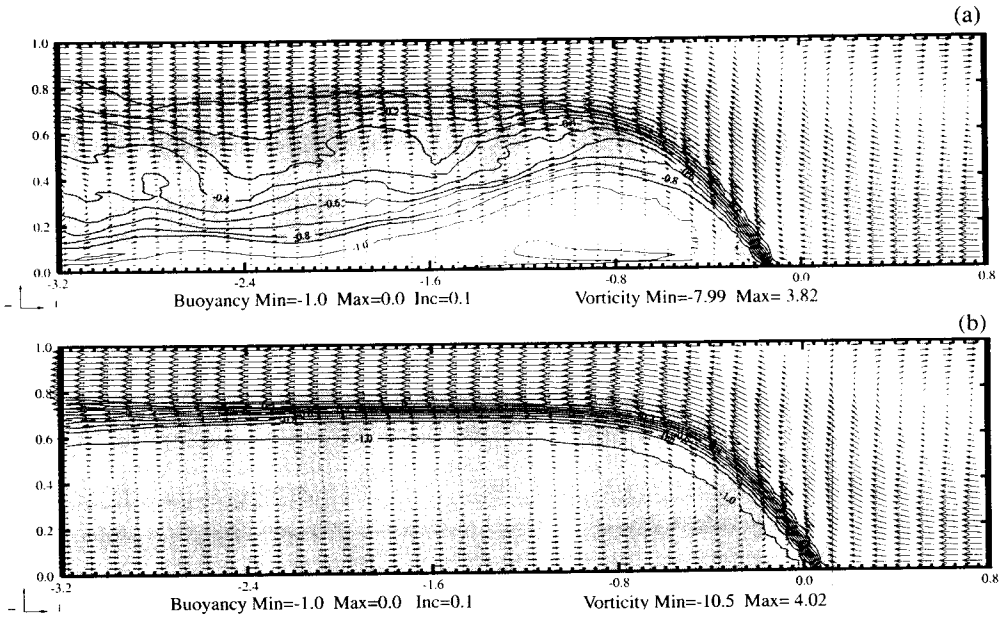

Figure 9. As Fig. 7 but for fields averaged over the period $T = 12$ to 18.

Figs. 10(a) and 11(a). In IC2P2, the lower layer in the cold pool has a positive shear/circulation and the upper layer has a negative shear. As a result, there exists a rear-to-front inflow jet at the mid-level of the cold pool, while the flow directly under the current interface has the same direction as the flow above. This configuration resembles the flow pattern in a mature squall line system. Based on the single-layer results seen earlier, one would expect a relatively smooth density interface due to the relatively small shear across the interface; this turns out not to be the case. As seen from the time evolution of the flow in Fig. 10, the upper negatively sheared layer in the cold pool appears to be dynamically unstable. Large KH eddies quickly develop along this shear layer and the density interface. The negative-vorticity-bearing air becomes wrapped into the vortices/eddies, and the less perturbed part of cold pool becomes dominated by the positive-vorticity-bearing air from the lower layer. This layer is apparently more stable, aided at least in part by the fixed lower boundary. As a result, the behaviour of the density current is mainly influenced by the direction of circulation in the lower (internal) shear layer. The time-averaged fields in Fig. 10(d) show several interesting features. First, the buoyancy gradient, originally concentrated in a single thin layer at the interface between the environmental flow and the cold-pool air, is now concentrated in two distinct zones—one between the negative-vorticity-bearing air and the environmental air above, and one separating the lower-layer positive circulation from the negative one above. Positive rear-to-front flow is concentrated in the second zone. As pointed out earlier, such a flow pattern resembles that in a mature squall line, where positive vorticity is generated baroclinically on the backside of the cold/heavy downdraught and is fed into the low-level rearward outflow, forming a circulation that is similar to the lower-layer positive circulation. Baroclinically generated negative vorticity along the frontal interface and that generated at the rear edge of the upper-level outflow contribute to the establishment of the upper negative circulation inside the (generalized) cold pool (Weisman 1992).

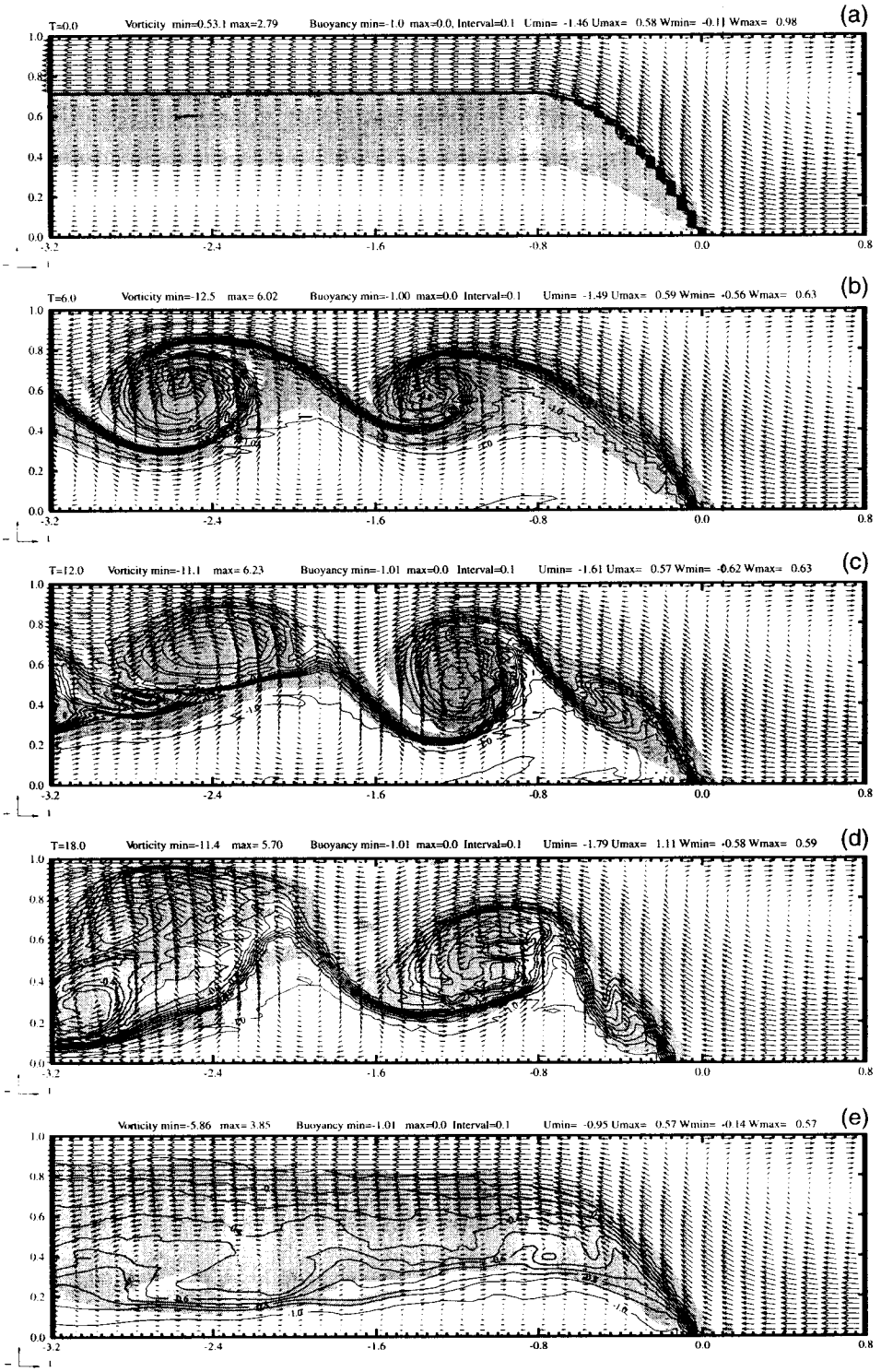

Figure 10. Non-dimensional velocity vector and buoyancy (contour) fields from experiment IC2P2 at time: (a) $T = 0$, (b) $T = 6$, (c) $T = 12$, (d) $T = 18$, and (e) averaged over the period from $T = 12$ to 18. The initial cold-pool circulation can be seen in (a). Areas with negative vorticity are shaded.

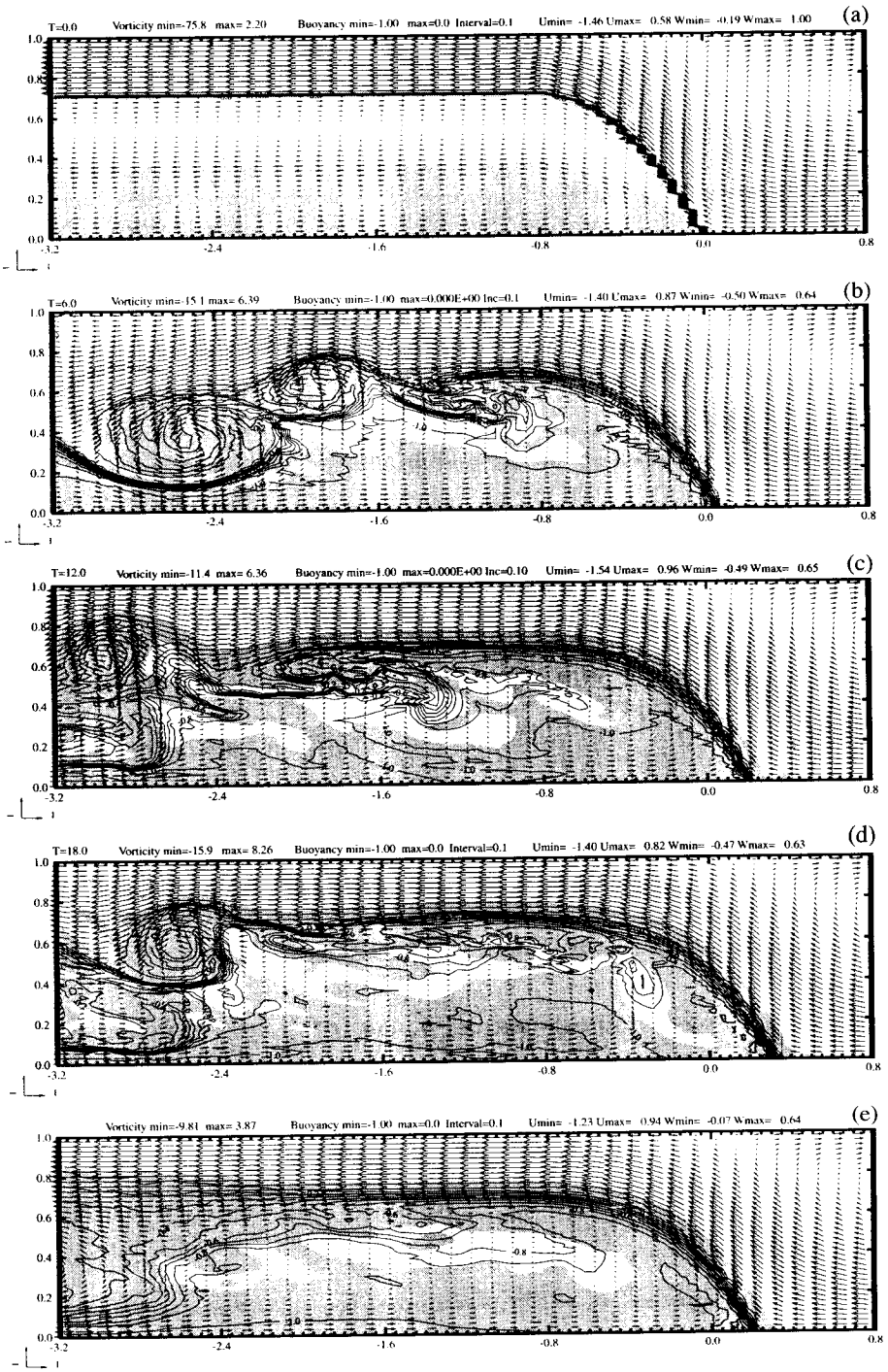

Figure 11. Same as Fig. 10 but for experiment IC2N2, in which the initial cold-pool circulations (shown in (a)) have opposite directions to those in IC2P2.

However, our present density current model does not attempt to fully address the issue of vorticity generation, the main goal here is to investigate the behaviour of the density current and the associated flows given an initial distribution of vorticity. Such distributions are idealizations of the more realistic situations, and are believed to be representative of the reality.

Finally, let us examine the results of experiment IC2N2, in which the initial cold-pool circulations are reversed in direction (Fig. 11(a)). Negative vorticity is found in the lower layer and positive vorticity between this layer and the density interface. By design, the shear across the interface is the same as in ICP1, in which large eddies develop along the interface due to strong KH instability. Figure 11 shows the time evolution and the time average of the flow. Interestingly, despite the large cross-interface shear, the interface becomes rather smooth at later times (e.g. $T = 18$), and the large-amplitude eddies are only found a distance of almost three from the frontal zone. The flow pattern resembles that of ICN1 more than ICP1. As in the previous case, the instability of, and the inability to maintain, the upper positive shear layer are obviously responsible for such behaviour. The lower-layer negative circulation is more stable and, with time, the head region of the cold pool becomes dominated by this negative circulation, which, together with the flow above the cold pool, sweeps the developing eddies along the interface rearward and establishes a more eddy-free density current interface. By $T = 18$, significant, though large in amplitude, eddies are only found about three length units behind the frontal zone, although some positive vorticity is still found inside the cold pool at this time. The interior flow at this time can perhaps be linked to fully developed rotor circulations in squall line systems. This situation is usually found in squall lines with significantly rearward-tilting updraughts and rearward-displaced downdraughts.

The results from the above two experiments show that the flow pattern inside a cold pool tends to be dominated by the circulation located near the ground, which is dynamically more stable. The behaviour of the density interface and density current head depends on more than just the cross-interface shear or the direction of circulation immediately below the interface.

5. Results from a high-resolution 2-D squall line simulation

To further illustrate the applicability of our density current models and the related simulation results to squall line dynamics, we present in this section the results from a high-resolution 2-D squall line simulation. A version of the ARPS (Xue *et al.* 1995, 2000, 2001) is used in a 2-D cloud model mode with Kessler-type warm-rain microphysics and order 1.5 subgrid-scale turbulence closure. A special feature used for this study is the synchronized flux-corrected transport scheme recently developed by the current author. When used to advect potential temperature, water vapour and the hydrometeor species together, the procedure of flux-correction synchronized for thermodynamic and microphysical variables results in better conservation of quantities such as equivalent potential temperature along air parcels, in addition to monotonicity (hence positive-definiteness of water variables). Ice processes, radiation, planetary boundary layer and land surface processes are neglected.

The computational domain is $500 \times 19.2\ \text{km}^2$. The vertical grid spacing is uniformly 100 m below 3 km, and is then stretched gradually to 500 m at the model top. The horizontal grid spacing is 200 m, a resolution significantly higher than that used by most simulation studies of this type. The convection is triggered by an initial elliptic thermal bubble that is 20 km in horizontal extent and 2.8 km in the vertical, centred 1.4 km above

ground and 200 km from the left boundary. In the figures to be presented, the centre of this initial bubble is marked as $x = 0$. Open lateral boundary conditions are employed. The top boundary is rigid and a Rayleigh damping layer is placed above 14 km.

The Weisman and Klemp (1982) analytical thermodynamic sounding is used, with the potential temperature and temperature set to 343 and 213 K, respectively, at the tropopause at 12 km height. Potential temperature at the surface is 300 K. Specific humidity is kept constant below 1.2 km at 15 g kg^{-1}.

The environmental wind profile has a constant 22.5 m s^{-1} speed below 2 km, and the speed is linearly reduced to zero at 3.285 km, and remains zero above. This profile is different from the typical low-level linear-shear profiles studied by TMM82, RKW88, Fovell and Ogura (1988) and others, and was previously examined by Xue (1990). The latter showed that such 'step' inflow profiles support long-lasting squall lines that tend to produce more precipitation than low-level linearly sheared profiles with similar total shear magnitude. In this paper, we focus our discussions on flow patterns near the cold pool or simulated squall line, and on the relevance of density current dynamics in a typical squall line system. First, the precipitation rate of the simulated squall line is plotted in a time–space diagram in Fig. 12. It can be seen that the overall system is quasi-steady, with new cells being continually re-generated at the leading edge of the cold pool and propagating to the left (at a typical speed of 14 m s^{-1}). The overall squall line system moves to the left at a speed of about 2.6 m s^{-1}, due to the unusually strong (22.5 m s^{-1}) low-level inflow.

In a similar manner to the density current investigation presented earlier, we perform an ensemble time average on the squall line fields, over a period of 1 h and centred on 10 h. Data were sampled at five-minute intervals and all fields were shifted in the horizontal direction before averaging so that the gust fronts collocate with that at 9.5 h. As shown by Fig. 12, this is a period when the system is rather steady (in the system-relative reference frame). The averaging (Fig. 13) removes most of the small-scale and transient signals, and accentuates the broader scales of flow. The instantaneous fields at 9.5 hours are shown in Fig. 14. The velocities shown are system relative.

The shading in Fig. 13(a) shows regions of relatively low equivalent potential temperature (θ_e). Because in most of the domain shown the air is saturated, as indicated by the simulated radar reflectivity contours, the θ_e contours give a good representation of the air parcel trajectories, and of streamlines in this quasi-steady case (again in the system-relative reference frame). It is clear that the cold pool consists of low-θ_e air that has been brought down from mid-levels to ground level by the downdraught circulation. This cold pool is separated by the updraught from the mid-level low-θ_e air ahead (to the right) of the squall line, in a similar way that the cold pool in the density current model is separated by the updraught from the mid-level upstream environmental flow (see e.g. Fig. 9). It can be seen that the air in the main updraught has similar θ_e values to those directly over the cold pool, in a manner that is similar to the lighter uniform-density fluid in the idealized two-fluid density current model (cf. Fig. 2 and Figs. 8–11). The main difference between the two is the presence of a layer of low-θ_e air at the mid-level ahead (to the right) of the main updraught found in the squall line system. However, since the air in this region has little vertical motion, the vertical distribution of regular buoyancy instead of θ_e is more relevant. The perturbation buoyancy field in Fig. 13(b) shows near-zero values in this region, therefore the dynamics of flow in the region is little different from that of neutrally stable flow in the idealized two-fluid density current model. Judging from the θ_e field, the 'generalized' cold pool exhibits a raised head of more than 5 km in depth. This is, however, still lower than that predicted by a steady-state density current model, and as a result we observe a density current

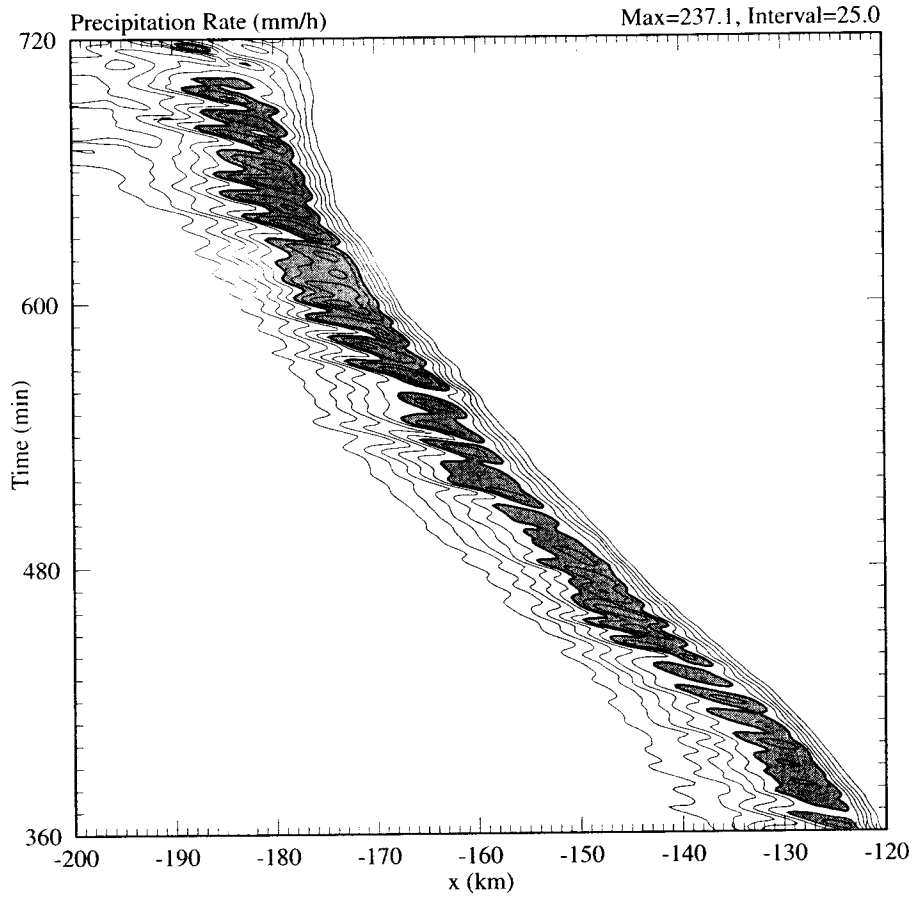

Figure 12. Time–space diagram of precipitation rate from the simulated squall line. Regions with rainfall rate exceeding 150 mm h^{-1} are shaded. Contour interval is 25 mm h^{-1}.

head with significant transient eddy activities (Fig. 14). This situation is also similar to density current experiment SLSA in XXD97 and experiment LID2 discussed earlier. The density current head as indicated by the buoyancy field (Fig. 13(b)) is about 3.5 km deep, shallower than that seen from the θ_e field.

Figure 13(c) shows that a zero- and positive-vorticity bearing updraught is separated from the cold pool and downdraught circulation by a slanting layer of negative vorticity. Most of this negative vorticity (shaded) is generated, through the horizontal buoyancy gradient (more clearly seen in Fig. 14(b)), along the cold pool–updraught frontal interface and at the upper levels on the left side of the positively buoyant updraught. The negative vorticity thus generated is transported rearward by the front-to-rear updraught branch of flow in the form of growing eddies, much like the KH eddies found in the density current simulations (Fig. 14(b)). Most of the positive vorticity in the downdraught branch is generated at the back edge of the cold pool, where the horizontal buoyancy gradient reverses direction (Figs. 13(c) and 14(c)). Overall, the flow pattern in the squall line system bears close similarities with those of two-fluid density currents with a near-ground cold-pool circulation that contains positive vorticity. In this regard, we can compare instantaneous vorticity and flow fields in Fig. 14(c) with those in Figs. 10(d) and

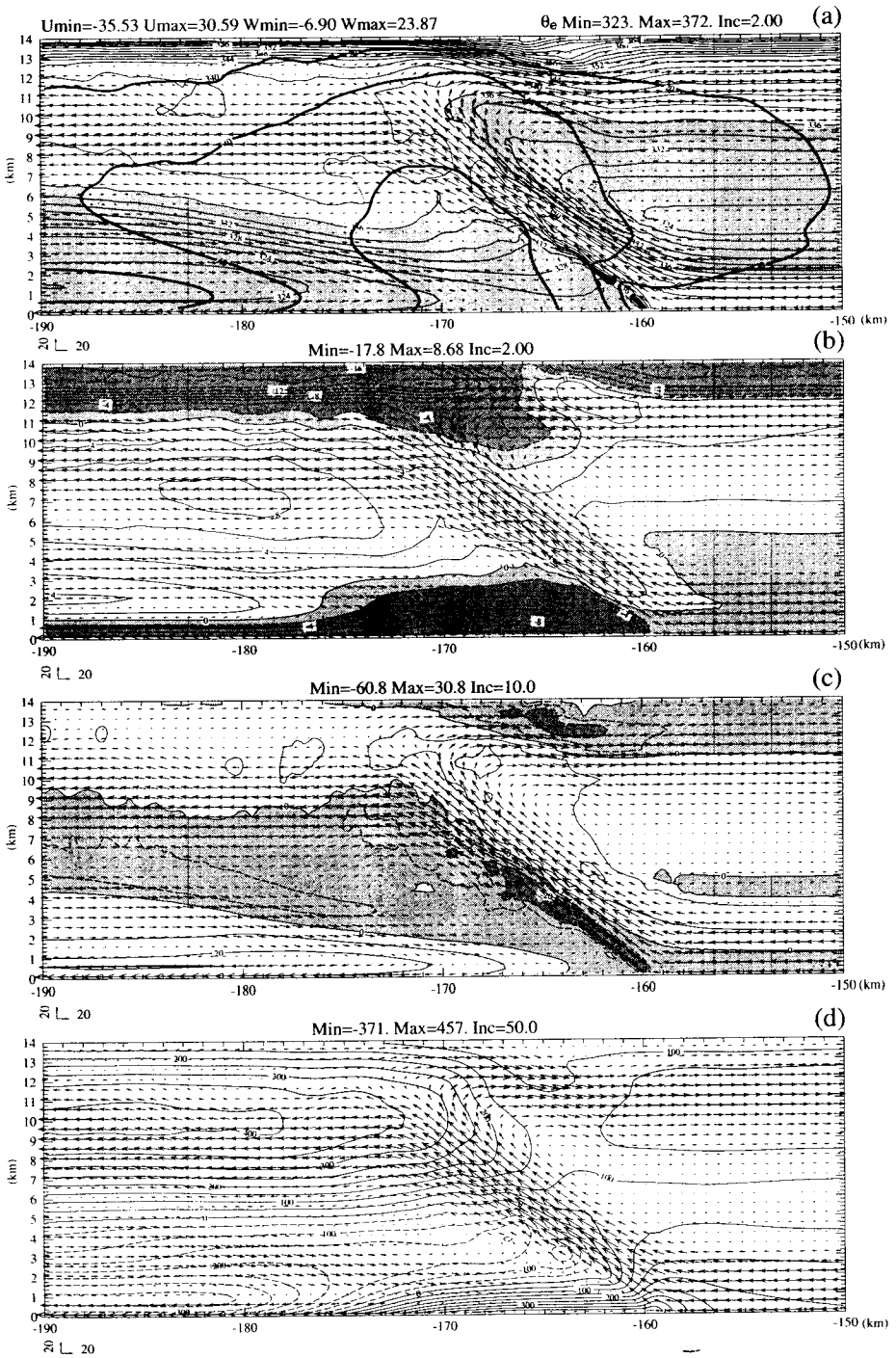

Figure 13. Fields from the simulated squall line averaged over a one-hour period at five-minute intervals. Wind vectors are plotted in all panels. (a) Equivalent potential temperature; values less than 336 K are shaded, thick lines are reflectivity contours at 20, 40 and 55 dBZ. (b) Temperature-equivalent perturbation-buoyancy (m s^{-2}) including water loading, with negatively buoyant areas lightly shaded and those colder than −2 K heavily shaded. (c) Vorticity (multiplied by 1000 s^{-1}), with negative areas lightly shaded and those less than −20 heavily shaded. (d) Perturbation pressure field (Pa). The figures are plotted to the physical scale, therefore the wind vectors show the actual direction of the flow.

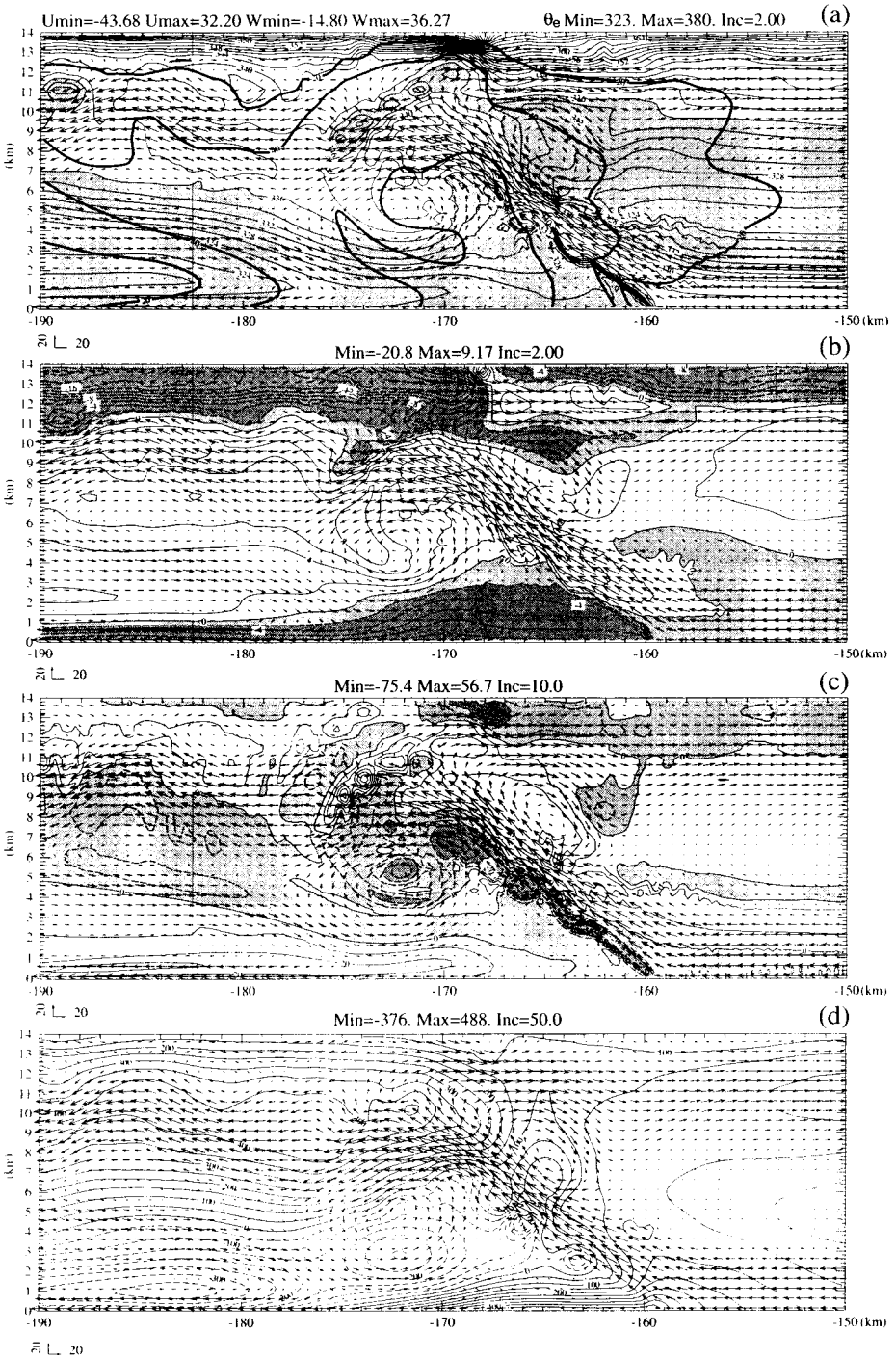

Figure 14. Same as Fig. 13 except for instantaneous fields at 9 h 30 min.

8(a), and the time-averaged fields in Fig. 13(c) with those in Figs. 10(e) and 9(a). The perturbation pressure field in Fig. 13(d) shows a pattern similar to those of simulated density currents, such as that in Fig. 6(b). The main difference is in the additional layer of positive pressure perturbations in the squall line that is associated with upper-level (above 7 km) convective outflow. It is the result of the hydrostatic response of the atmosphere to condensational heating. Finally, we point out that the updraught of a simulated squall line has an orientation close to 45° at the mid-levels, and the gust front is at an angle close to 60° to the horizontal direction at the surface.

6. Summary and discussion

In this paper, the effect of the imposed rigid lid in the idealized density current models developed in previous studies is examined. It is shown, through numerical experiments, that a stable layer located at and above the level of an original rigid lid acts in a similar way to the rigid lid. The slightly decreased channelling effect above the density current due to the raised base of the stable layer tends to be offset by the effect of the increased channel depth. For the particular density current and inflow configuration considered, the simulated density current has an almost identical depth to that obtained under a rigid lid. The density current propagates slightly faster than the latter case. The behaviour of the density current is very different if the stable layer is also removed. All of these results can still be adequately explained by the theoretical model with a rigid lid, through the rescaling of parameters based on the new effective channel depth. These results support our previous suggestions that, in the atmosphere, the tropopause or a tropospherical inversion layer acts in a similar way to the rigid lid found in our idealized density current models, and the results of these models are applicable to organized quasi 2-D convection systems in the atmosphere.

The effects of cold-pool internal circulations in simulated density currents are also examined. When a single circulation is present inside the cold pool, the direction of circulation that gives rise to a smaller shear across the density interface leads to a smoother interface and a much more steady density current head. Large-amplitude eddies develop along the interface when the circulation is reversed. When two shear layers are initially present inside the cold pool, the flow pattern inside the cold pool tends to be dominated by the circulation located near the ground, which is dynamically more stable. The behaviour of the density interface and the density current head depend not solely on the cross-interface shear or the direction of circulation directly below the interface as suggested by the single circulation results. The overall flow pattern in the density current in which the cold-pool circulation contains rearward flows at ground level bears a close similarity with that found in a mature squall line system, as is shown through the comparison with a simulated squall line presented in this paper. It is argued that the density current in a squall line can be viewed in terms of the equivalent potential temperature, and such a generalized density current can reach a depth of 5 km or more. Studies of density currents in sheared flows in idealized models can help us to understand the fundamental flow dynamics in squall lines, in particular, the interaction of shear inflow with the cold pool.

Acknowledgements

This research was supported by NSF ATM-9909007, and by NSF Grant ATM91-20009 to the Center for Analysis and Prediction of Storms (CAPS). It was also partially supported by a Junior Faculty Research grant from the University of Oklahoma. Figures

were produced using the ZXPLOT graphics package developed by the author. The author benefited from discussions with Drs Qin Xu and Kelvin Droegemeier, and thanks Dr Mitchell Moncrieff and an anonymous reviewer for their constructive comments.

REFERENCES

Atkins, N. T., Weckwerth, T. M. and Wakimoto, R. M. 1995 Observations of the sea-breeze front during CAPE. Part II: Dual Doppler and aircraft analysis. *Mon. Weather Rev.*, **123,** 944–969

Benjamin, T. B. 1968 Gravity currents and related phenomena. *J. Fluid Mech.*, **31,** 209–248

Carbone, R. E. 1982 A severe frontal rainband. Part I: Stormwide hydrodynamic structure. *J. Atmos. Sci.*, **39,** 258–279

Fovell, R. G. and Ogura, Y. 1988 Numerical simulation of a midlatitude squall line in two dimensions. *J. Atmos. Sci.*, **45,** 3846–3879

Houze, R. A. Jr. 1989 Observed structure of mesoscale convective systems and implications for large-scale heating. *Q. J. R. Meteorol. Soc.*, **115,** 425–462

Liu, C.-H. and Moncrieff, M. W. 1996a An analytical study of density currents in sheared, stratified flow and the effects of latent heating. *J. Atmos. Sci.*, **53,** 3303–3312

1996b A numerical study of the effects of ambient flow and shear on density currents. *Mon. Weather Rev.*, **124,** 2282–2303

Moncrieff, M. W. 1978 The dynamical structure of two-dimensional steady convection in constant vertical shear. *Q. J. R. Meteorol. Soc.*, **104,** 543–567

1992 Organized mesoscale convective systems: Archetypal dynamical models, mass and momentum flux theory and parametrization. *Q. J. R. Meteorol. Soc.*, **118,** 819–850

Moncrieff, M. W. and So, D. K. 1989 A hydrodynamic theory of conservative bounded density currents. *J. Fluid Mech.*, **198,** 177–197

Rotunno, R., Klemp, J. B. and Weisman, M. L. 1988 A theory for strong long-lived squall lines. *J. Atmos. Sci.*, **45,** 463–485

Simpson, J. E., Mansfield, D. A. and Milford, J. R. 1977 Inland penetration of sea-breeze fronts. *Q. J. R. Meteorol. Soc.*, **103,** 47–76

Thorpe, A. J., Miller, M. J. and Moncrieff, M. W. 1982 Two-dimensional convection in non-constant shear: A model of midlatitude squall lines. *Q. J. R. Meteorol. Soc.*, **108,** 739–762

von Karman, T. 1940 The engineer grapples with nonlinear problems. *Bull. Am. Math. Soc.*, **46,** 615–683

Weckworth, T. M. and Wakimoto, R. 1992 The initiation and organization of convective cells atop a cold-air outflow boundary. *Mon. Weather Rev.*, **120,** 2169–2187

Weisman, M. L. 1992 The role of convectively generated rear-inflow jets in the evolution of long-lived mesoconvective systems. *J. Atmos. Sci.*, **49,** 1826–1847

Weisman, M. L. and Klemp, J. B. 1982 The dependence of numerically simulated convective storms on vertical wind shear and buoyancy. *Mon. Weather Rev.*, **110,** 504–520

Xu, Q. 1992 Density currents in shear flows—A two-fluid model. *J. Atmos. Sci.*, **49,** 511–524

Xu, Q. and Moncrieff, M. W. 1994 Density current circulations in shear flows—A two-fluid model. *J. Atmos. Sci.*, **51,** 434–446

Xu, Q., Chang, F. S. and Lou, C. P. 1992 Finite element solutions of free-interface density currents. *Mon. Weather Rev.*, **120,** 230–233

Xu, Q., Xue, M. and Droegemeier, K. K. 1996 Numerical simulations of density currents in sheared environments within a vertically confined channel. *J. Atmos. Sci.*, **53,** 770–786

Xue, M. 1990 'Towards the environmental condition for long-lived squall lines: Vorticity versus momentum'. Pp. 24–29 in Preprint of the AMS 16th conference on severe local storms, Alberta, Canada. American Meteorological Society, Boston, USA

2000 Density current in two-layer shear flows. *Q. J. R. Meteorol. Soc.*, **126,** 1301–1320

Xue, M., Droegemeier, K. K., Wong, V., Shapiro, A. and Brewster, K. 1995 'ARPS version 4.0 user's guide'. Available from Center for Analysis and Prediction of Storms, University of Oklahoma, 100 E. Boyd St., Norman, OK 73019, USA